

Cite this: DOI: 10.1039/c0xx00000x

www.rsc.org/xxxxxx

Structure-Based Drug Design of Chromone Antagonists of the Adenosine A_{2A} Receptor

Stephen P. Andrews,^{*a} Jonathan S. Mason,^a Edward Hurrell^a and Miles Congreve^a

Received (in XXX, XXX) Xth XXXXXXXXXX 20XX, Accepted Xth XXXXXXXXXX 20XX

DOI: 10.1039/b000000x

The structure-guided optimisation of a hit series of chromone derivatives, previously identified using virtual screening of homology models of the adenosine A_{2A} receptor, has led to the discovery of potent, selective and ligand efficient antagonists. Lipophilic hotspots and calculated water networks were modelled within the receptor binding site to facilitate rational ligand design.

High resolution crystal structures have been published for twenty G protein-coupled receptors (GPCRs), including 17 members of the rhodopsin family, a frizzled receptor and two members of the secretin family.¹⁻⁴ These advances in structural biology have given enormous insight into the binding sites of this superfamily of receptors, facilitating structure-based drug design and providing templates for the construction of high confidence homology models.^{5,6}

The adenosine A_{2A} receptor is a member of the rhodopsin family of GPCRs. Many ligands are known for this receptor, including a number of antagonists which have been investigated clinically for the treatment of CNS disorders, particularly Parkinson's disease.⁷ For example, preladenant reached phase 3 clinical trials but has recently been discontinued owing to lack of efficacy versus placebo. Currently there are no marketed A_{2A} receptor antagonists and exploration of further chemotypes is warranted.

Compound **1** was previously reported as a 2.0 μM hit following the virtual screening of homology models of the A_{2A} receptor which were built from the crystal structure of the β₁ adrenergic receptor.⁸ Herein we describe the efficient optimisation of a

series of chromone ligands with structure-based approaches driven by molecular modelling and biophysical techniques.

Compound **1** was identified prior to solving the X-ray crystal structure of the A_{2A} receptor; however, there are now multiple 3D structures available for this receptor, which has been solved in both its active and inactive forms,⁹ facilitated by either a fusion protein¹⁰ or thermostabilisation technology.¹¹

Initial analysis of **1** with the A_{2A} receptor homology models resulted in two putative binding modes, A and B (figure 1) from Glide¹² docking studies. In order to improve the activity of **1** by rational design it was first necessary to validate binding mode A which, after further modelling and careful analysis, appeared to be the most plausible. To this end, small sets of analogues were designed iteratively and tested in a competitive radioligand binding assay¹³ with hA_{2A} receptor and [³H]-ZM241385.

Initially, the negatively charged carboxylate functionality was removed from **1** as it had been modelled to sit unfavourably in a lipophilic region lined by Leu167^{ECL2}, Ile66^{2,64} and Met270^{7,35,14}. As predicted, replacement with a positively charged group such as an aliphatic amine (**2**) did not invoke an increase in affinity, whereas conversion to a neutral group such as an ester (**3**) gave rise to a 20-fold improvement in affinity (table 1).

Modifications with simple alkyl groups led to improvements in ligand efficiency¹⁵ (**4**, LE = 0.42), and larger chains were also well tolerated (**5**, pK_i = 7.6). A simple acetate group at position R¹ was found to maintain a good level of affinity (**6**) and the unsubstituted hydroxyl derivative (**7**) showed the highest LE (0.47). This phenol group was kept constant in the following round of design where the effects of substituents at other

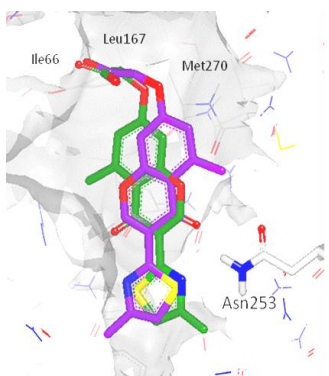
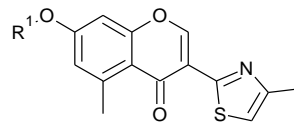


Fig. 1 Putative binding modes of compound **1**. In mode A (green carbon) the thiazole N hydrogen bonds to Asn253 and in mode B (purple carbon) the chromone carbonyl group hydrogen bonds to Asn253.

Table 1 Investigation of substituents at position R¹.

	R ¹	pK _i	LE
1	-CH ₂ CO ₂ H	5.7	0.34
2	-(CH ₂) ₂ NMe ₂	5.8	0.33
3	-CH ₂ CO ₂ Et	7.0	0.38
4	-methylcyclopropyl	7.1	0.42
5	-(CH ₂) ₃ C≡CH	7.6	0.43
6	-CH ₂ C(=O)Me	7.5	0.46
7	-H	6.5	0.47



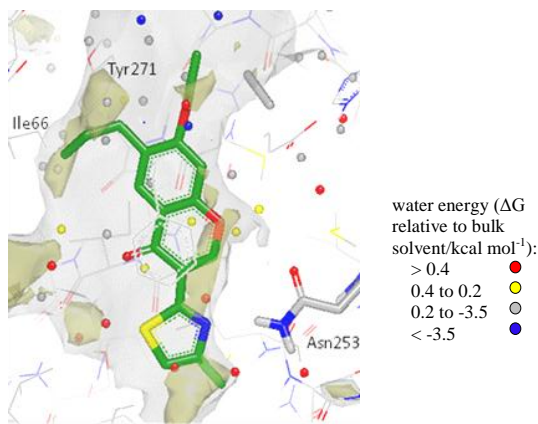


Fig. 2 Compound **10** in binding mode A; GRID C3 surface (1.0 kcal mol⁻¹; grey) and C1= lipophilic hotspots (-2.8 kcal mol⁻¹; yellow) for A_{2A} receptor; and WaterMap waters calculated for the pseudo-apo protein from the ligand complex PDB: 3UZC.

positions on the chromone scaffold were rationally explored. During a druggability analysis,⁶ a lipophilic hotspot was identified with a GRID aromatic CH (C1=) probe,¹⁶ in a pocket lined by Ile66^{2,64} and Tyr271^{7,36} (figure 2). This led to the design of compounds with lipophilic groups at the vector defined by R² (C-6 of the chromone core), with the minimum chain length of two atoms required to reach the hotspot (table 2). When compared to the R²-unsubstituted derivative (**8**), compounds **9**, **10** and **11** all showed very good affinities for the receptor. The size of the lipophilic hotspot indicated that a propyl group would most efficiently fill this pocket and this was indeed found to be the case, with **10** showing the highest LE. A later analysis using WaterFLAP and WaterMap in conjunction with A_{2A} receptor crystal structures showed that moderately high energy or ‘unhappy’ waters⁶ are in this region and are displaced by **10** (see supplementary information). The larger *n*-pentyl derivative (**11**) explores areas outside of the hotspot and shows only a small increase in potency when compared to **10**. Compounds **9** and **10** were therefore progressed in preference to **11** as they showed the best balance of LE and lipophilic ligand efficiency¹⁷ (LLE = 3.6, 3.7 and 2.8, respectively).

The proposed binding mode A was further confirmed by testing compound **12** with a methyl substituent at position R³. Compound **12** was predicted to impose a steric clash on Asn253^{6,55} in binding mode A (the carbon at position C-2 of the chromone is almost at the GRID C3 surface – see figure 2), and was found to be four times less active than **8**. By contrast, in

Table 2 Investigation of substituents at vectors R² and R³.

	R ²	R ³	pK _i	LE
8	H	H	5.7	0.44
9	Et	H	7.1	0.49
10	<i>n</i> -Pr	H	7.6	0.50
11	<i>n</i> -pentyl	H	7.7	0.46
12	H	Me	5.1	0.37

binding mode B, the methyl group of **12** faces a large pocket and a minimal change of activity would be expected (see figure 1).

Combining the SAR observed in tables 1 and 2 led to compound **13** which maintained a high LE (0.48) and was found to have a good affinity for the A_{2A} receptor (pK_i = 8.5; figure 3). Subsequent Biophysical MappingTM (BPM – a technique which combines site-directed mutagenesis with surface plasmon resonance screening in order to determine the individual contributions of binding site residues to the binding of ligands)¹⁸ analysis of **13** suggested that the propyl group of this ligand interacted with Ile66^{ECL2} and Tyr271^{7,36}, which further supports binding mode A, in which the chromone C-6 substituent is projected towards this lipophilic sub-pocket of the binding site.⁸

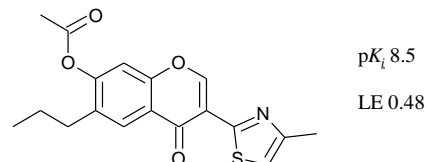


Fig. 3 Compound **13**.

The compelling evidence of the BPM studies and the modelling presented here were later corroborated by X-ray crystallography data from a co-crystal of a derivative from this series bound to thermostabilised A_{2A} receptor (StaR).^{8,13} The electron density of this relatively low resolution structure (unpublished data) was used to confirm and fine tune the ligand complex.

Screening selected analogues vs the A₁ receptor revealed that the series shows a higher binding affinity for the A_{2A} receptor, with several examples showing >100-fold selectivity. For example, compounds **6** and **13** were 13- and 16-fold selective, respectively, and compounds **4**, **9** and **11** were all >100-fold selective.

The final area of the molecules to be investigated was the 4-methylthiazole group. The N atom of this heterocycle provides the core H-bond found for A_{2A} receptor ligands to Asn253^{6,55}. Furthermore, the methyl group at the 4 position of this heterocycle makes a crucial contribution to the binding affinity of this series of molecules, with a severe (33-fold) loss of activity upon its removal (**15**→**16**). This is a clear example of a ‘magic methyl’ effect, and is of similar magnitude to a recent example

Table 3 Investigation of the methylthiazole substituent.

	R ⁴	R ⁵	pK _i	LE
14	Me		7.5	0.43
15	H		7.3	0.43
16	H		5.8	0.36

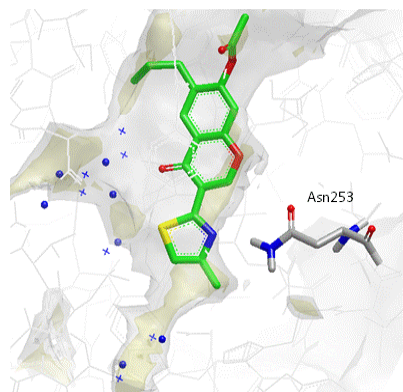


Fig. 4 Waters in the proximity of the thiazole ring from the computed water networks for **13** (blue spheres, ligand shown) and **14** (blue crosses) from a WaterFLAP analysis used to compare water network perturbation.

published with opioid receptor antagonists,¹⁹ but here there is a clear structural understanding of its origin. The methyl group displaces an ‘unhappy’ water (red sphere in figure 2), identified from a WaterMap calculation of the water network and energetics for the pseudo-apo X-ray structure from PDB:3UZC.^{6:13} This water is in a lipophilic hotspot cavity in the binding site, giving a strong beneficial effect; furthermore, without the thiazole methyl group, this water would be trapped in an even more unfavourable position (owing to the remaining apolar CH of the ligand), that would bind less deeply or create a ‘dewetted’ vacuum region.

The power of water network energetic analyses to rationalise SAR and drive design is further illustrated when changing the position of the sulphur atom within the thiazole ring. A ten-fold reduction in activity is found between compounds **13** and **14** (Table 3), yet no changes in favourable interactions or steric clashes are observed with the receptor. Both ligands are still able to hydrogen bond to Asn253^{6,55} via their N atoms. Scoring of the two isomers using the docking program Glide in both SP and XP modes showed non-significant differences (approx. 0.1 kcal better or worse, respectively) and no differences were observed in a rescoring with Hyde²⁰ that explicitly considers hydrophobic interactions via atom logP contributions. The significant difference in potency observed with this small change of an indirectly-interacting ligand atom can be rationalized by analysing the computed energies of the waters in the bottom (affected in **14** by the S atom) and the left (affected in **13** by the S atom) of the pocket (figure 4). Using the sum of the energies of the GRID probes for water and C1= in WaterFLAP, the 2 waters at the bottom were found to increase in energy by 9 kcal (**13**→**14**), whereas the 5 waters to the left were only 4.5 kcal lower. The significant increase in the total energy of the waters affected by **13**→**14** could thus rationalise the potency drop.

In summary, the structure-guided optimization of a chromone hit series has led to the discovery of potent antagonists of the A_{2A} receptor with high LE. Important aspects of the series’ SAR can be explained by the effect of displacing waters from lipophilic hotspots (‘unhappy’ waters) or by perturbing the calculated water network within the binding site. This study is an example of how high quality GPCR binding mode information is starting to significantly impact on the discovery of new agents for this important class of receptors. In particular, the ability to consider the position and energy of lipophilic hotspots and of calculated water molecules offers great promise for rational drug design.

Notes and references

- ^a Heptares Therapeutics Ltd., Biopark, Broadwater Road, Welwyn Garden City, AL7 3AX, United Kingdom. * Corresponding author steve.andrews@heptares.com. © Heptares Therapeutics 2013. The HEPTARES name is a trade mark of Heptares Therapeutics Ltd.
- † Electronic Supplementary Information (ESI) available: synthesis procedures & computational methods. See DOI: 10.1039/b000000x/
1. N. Bertheleme, P. S. Chae, S. Singh, D. Mossakowska, M. M. Hann, K. J. Smith, J. A. Hubbard, S. J. Dowell, and B. Byrne, *Biochim.Biophys.Acta*, 2013, **1828**, 2583.
 2. C. Wang, H. Wu, V. Katritch, G. W. Han, X. P. Huang, W. Liu, F. Y. Siu, B. L. Roth, V. Cherezov, and R. C. Stevens, *Nature*, 2013, **497**, 338.
 3. K. Hollenstein, J. Kean, A. Bortolato, R. K. Cheng, A. S. Dore, A. Jazayeri, R. M. Cooke, M. Weir, and F. H. Marshall, *Nature*, 2013, **499**, 438.
 4. F. Y. Siu, M. He, G. C. de, G. W. Han, D. Yang, Z. Zhang, C. Zhou, Q. Xu, D. Wacker, J. S. Joseph, W. Liu, J. Lau, V. Cherezov, V. Katritch, M. W. Wang, and R. C. Stevens, *Nature*, 2013, **499**, 444.
 5. B. Kobilka, *Angew.Chem.Int.Ed Engl.*, 2013.
 6. J. S. Mason, A. Bortolato, M. Congreve, and F. H. Marshall, *Trends Pharmacol.Sci.*, 2012, **33**, 249.
 7. J. F. Chen, H. K. Eltzschig, and B. B. Fredholm, *Nat.Rev.Drug Discov.*, 2013, **12**, 265.
 8. C. J. Langmead, S. P. Andrews, M. Congreve, J. C. Errey, E. Hurrell, F. H. Marshall, J. S. Mason, C. M. Richardson, N. Robertson, A. Zhukov, and M. Weir, *J.Med.Chem.*, 2012, **55**, 1904.
 9. S. P. Andrews and B. Tehan, *Med.Chem.Commun.*, 2013, **4**, 52.
 10. E. Chun, A. A. Thompson, W. Liu, C. B. Roth, M. T. Griffith, V. Katritch, J. Kunken, F. Xu, V. Cherezov, M. A. Hanson, and R. C. Stevens, *Structure.*, 2012, **20**, 967.
 11. N. Robertson, A. Jazayeri, J. Errey, A. Baig, E. Hurrell, A. Zhukov, C. J. Langmead, M. Weir, and F. H. Marshall, *Neuropharmacology*, 2011, **60**, 36.
 12. T. A. Halgren, R. B. Murphy, R. A. Friesner, H. S. Beard, L. L. Frye, W. T. Pollard, and J. L. Banks, *J.Med.Chem.*, 2004, **47**, 1750.
 13. M. Congreve, S. P. Andrews, A. S. Dore, K. Hollenstein, E. Hurrell, C. J. Langmead, J. S. Mason, I. W. Ng, B. Tehan, A. Zhukov, M. Weir, and F. H. Marshall, *J.Med.Chem.*, 2012, **55**, 1898.
 14. Superscript numbers refer to Ballesteros-Weinstein notation: J. A. Ballesteros, H. Weinstein, and C. S. Stuart, in *Methods in Neurosciences*, Academic Press, New York, 1995, vol. 25, p. 366.
 15. A. L. Hopkins, C. R. Groom, and A. Alex, *Drug Discov.Today*, 2004, **9**, 430.
 16. P. J. Goodford, *J.Med.Chem.*, 1985, **28**, 849.
 17. P. D. Leeson and B. Springthorpe, *Nat.Rev.Drug Discov.*, 2007, **6**, 881.
 18. A. Zhukov, S. P. Andrews, J. C. Errey, N. Robertson, B. Tehan, J. S. Mason, F. H. Marshall, M. Weir, and M. Congreve, *J.Med.Chem.*, 2011, **54**, 4312.
 19. G. Lunn, B. J. Banks, R. Crook, N. Feeder, A. Pettman, and Y. Sabnis, *Bioorg.Med.Chem.Lett.*, 2011, **21**, 4608.
 20. N. Schneider, S. Hindle, G. Lange, R. Klein, J. Albrecht, H. Briem, K. Beyer, H. Claussen, M. Gastreich, C. Lemmen, and M. Rarey, *J.Comput.Aided Mol.Des*, 2012, **26**, 701.